

## Electronic Supplementary Information

### Ultrafine CoO nanoparticles as an efficient cocatalyst for enhanced photocatalytic hydrogen evolution

Jiayu Chu,<sup>a</sup> Guoji Sun,<sup>b</sup> Xijiang Han,<sup>\*a</sup> Xin Chen,<sup>c</sup> Jiajun Wang,<sup>a</sup> Wen Hu,<sup>d</sup> Iradwikanari Waluyo,<sup>d</sup> Adrian Hunt,<sup>d</sup> Yunchen Du,<sup>a</sup> Bo Song,<sup>\*e</sup> and Ping Xu<sup>\*a</sup>

<sup>a</sup> MIIT Key Laboratory of Critical Materials Technology for New Energy Conversion and Storage, School of Chemistry and Chemical Engineering, Harbin Institute of Technology, Harbin 150001, China.

<sup>b</sup> State Key Laboratory of Advanced Welding and Joining, Harbin Institute of Technology, Shenzhen Graduate School, Shenzhen 518055, China.

<sup>c</sup> School of Advanced Materials, Peking University, Shenzhen Graduate School, Shenzhen 518055, China.

<sup>d</sup> National Synchrotron Light Source II, Brookhaven National Laboratory, Upton, NY 11973, USA.

<sup>e</sup> Academy of Fundamental and Interdisciplinary Sciences, Harbin Institute of Technology, Harbin 150001, China.

\*Corresponding authors. E-mail: pxu@hit.edu.cn (P.X.); hanxijiang@hit.edu.cn (X.H.); songbo@hit.edu.cn (B.S.).

Tel: +86-(451)-86418750; fax: +86-(451)-86413702.

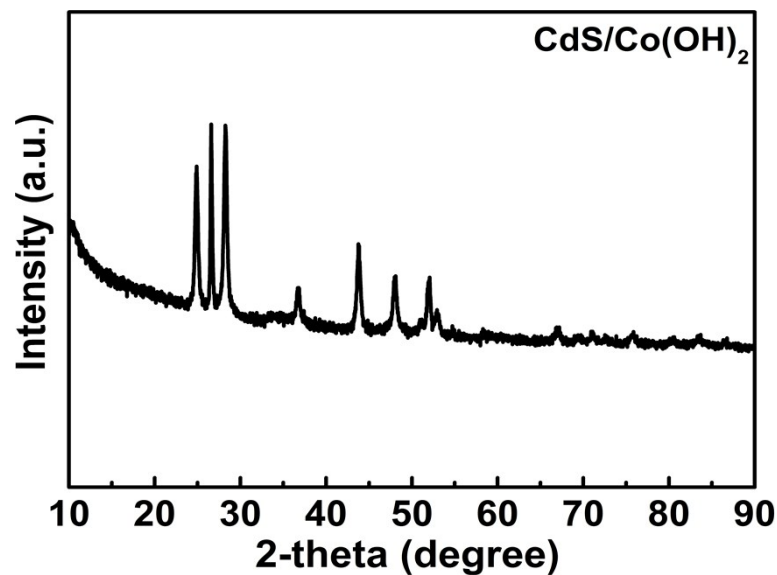


**Fig. S1.** XRD pattern of the CdS/Co(OH)<sub>2</sub> nanocomposites. The diffraction peaks can be well indexed to the standard hexagonal CdS phase (JCPDS No.41-1049). Diffraction peaks of Co(OH)<sub>2</sub> are not detected due to its amorphous feature.

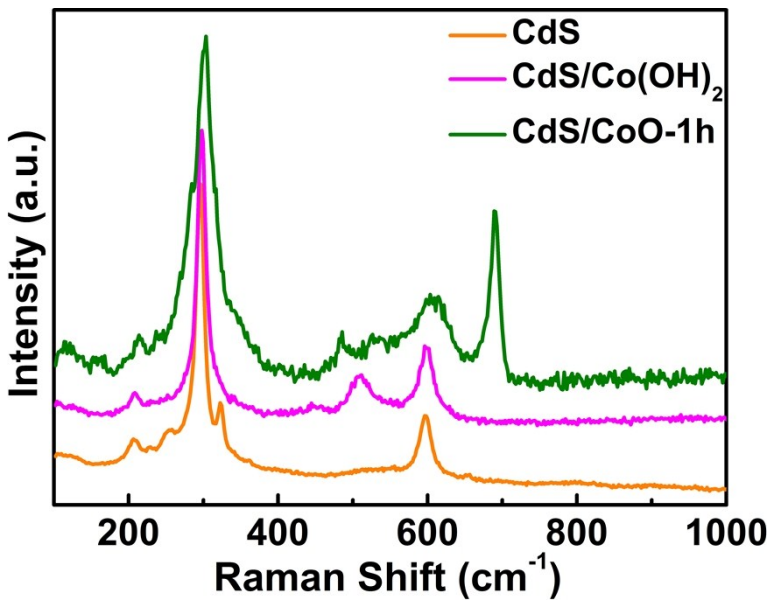


**Fig. S2.** Raman spectra of CdS, CdS/Co(OH)<sub>2</sub> nanocomposites and CdS/CoO-1h heterostructures. The characteristic peaks at 296 and 598 cm<sup>-1</sup> in the Raman spectra are identified as the CdS,<sup>1</sup> where the Raman bands at 453 and 515 cm<sup>-1</sup> can be ascribed to Co(OH)<sub>2</sub>, indicating the presence of Co(OH)<sub>2</sub>.<sup>2</sup> While, the peaks at 485, 530 and 690 cm<sup>-1</sup> are in good agreement with the CoO,<sup>3, 4</sup> which further proves that the CdS/CoO heterostructures is prepared successfully.

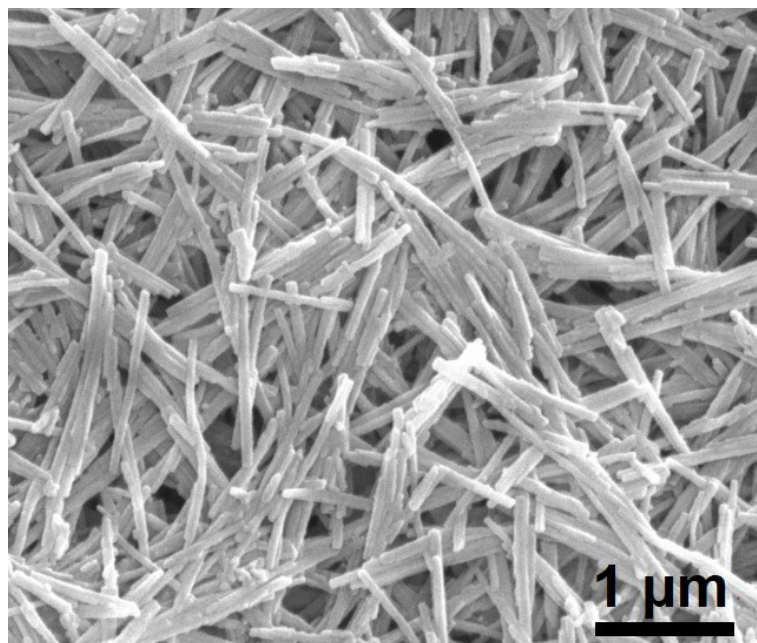


**Fig. S3.** SEM image of the as-prepared CdS nanorods.

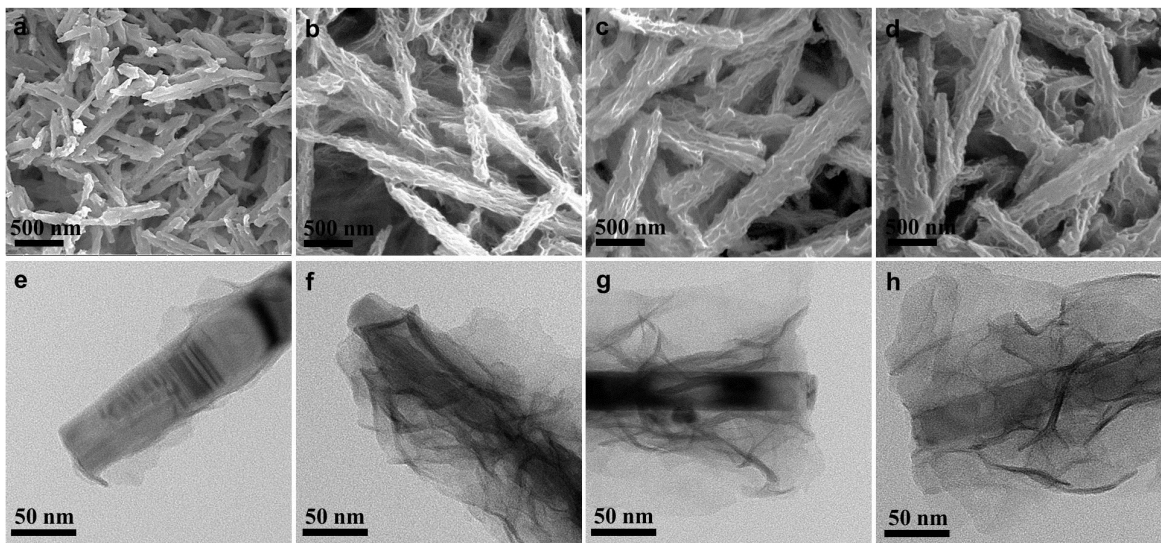


**Fig. S4.** SEM images and corresponding TEM images of the prepared (a, e) CdS/Co(OH)<sub>2</sub>-0.25 h, (b, f) CdS/Co(OH)<sub>2</sub>-1 h, (c, g) CdS/Co(OH)<sub>2</sub>-3 h and (d, h) CdS/Co(OH)<sub>2</sub>-6 h. It is clearly seen that with prolonged reaction time period, more amorphous Co(OH)<sub>2</sub> nanosheets can be formed on the CdS nanorods.

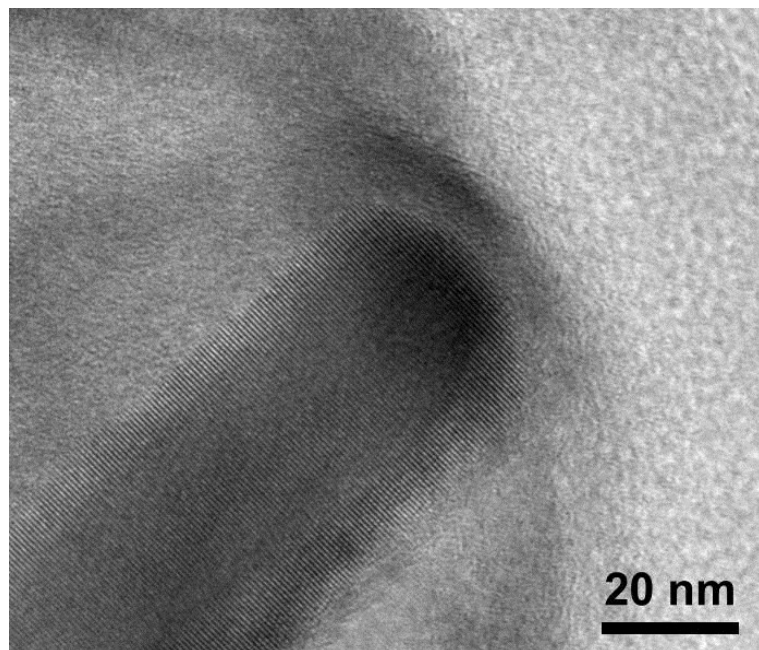


**Fig. S5.** TEM image of CdS/Co(OH)<sub>2</sub>-1h nanocomposites, which shows the highly crystallized CdS nanorod is wrapped by amorphous Co(OH)<sub>2</sub>.

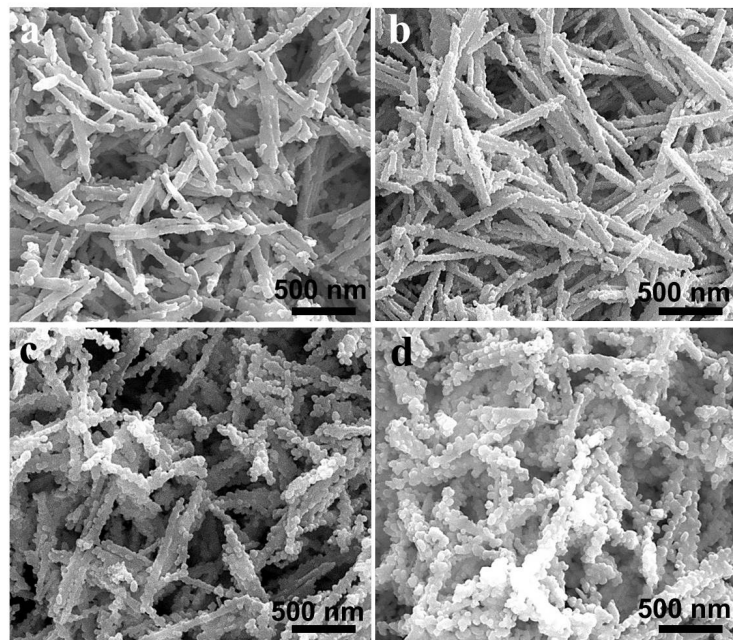


**Fig. S6.** SEM images of the prepared (a) CdS/CoO-0.25 h, (b) CdS/CoO-1 h, (c) CdS/CoO-3 h and (d) CdS/CoO-6 h.

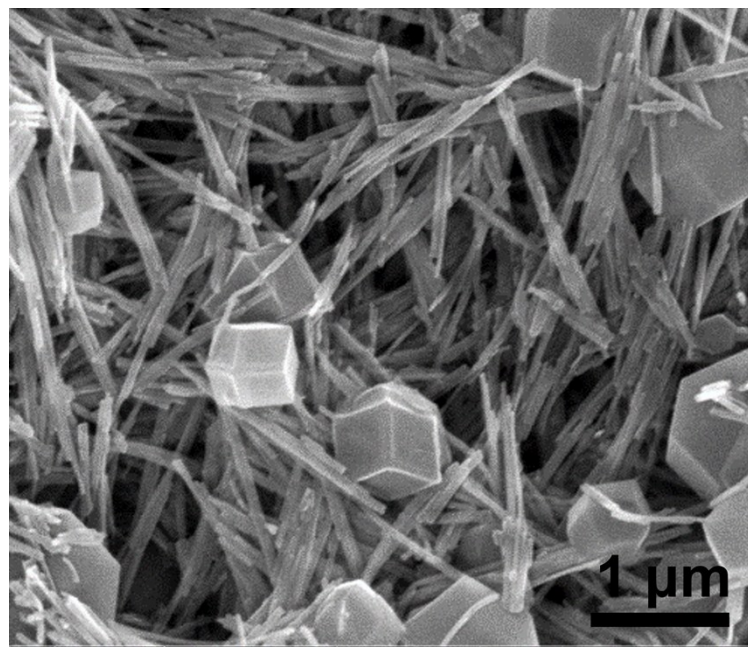


**Fig. S7.** SEM image of CdS/ZIF-67 mixture prepared with the molar ratio of  $\text{Co}^{2+}$  ions to 2MIM at ~1:7.

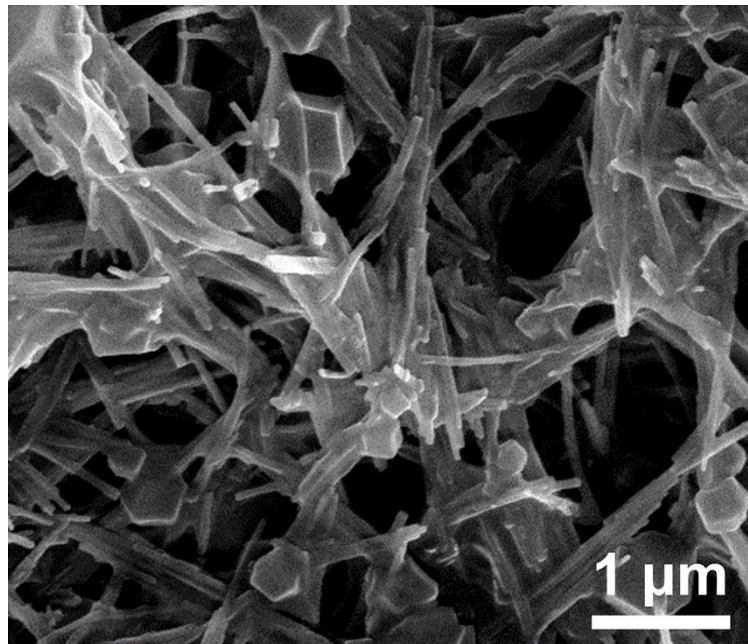


**Fig. S8.** SEM image of a critical structure for CdS/ZIF-67 mixture and CdS/Co(OH)<sub>2</sub> nanocomposites prepared with the molar ratio of Co<sup>2+</sup> ions to 2MIM at ~1:1.4.

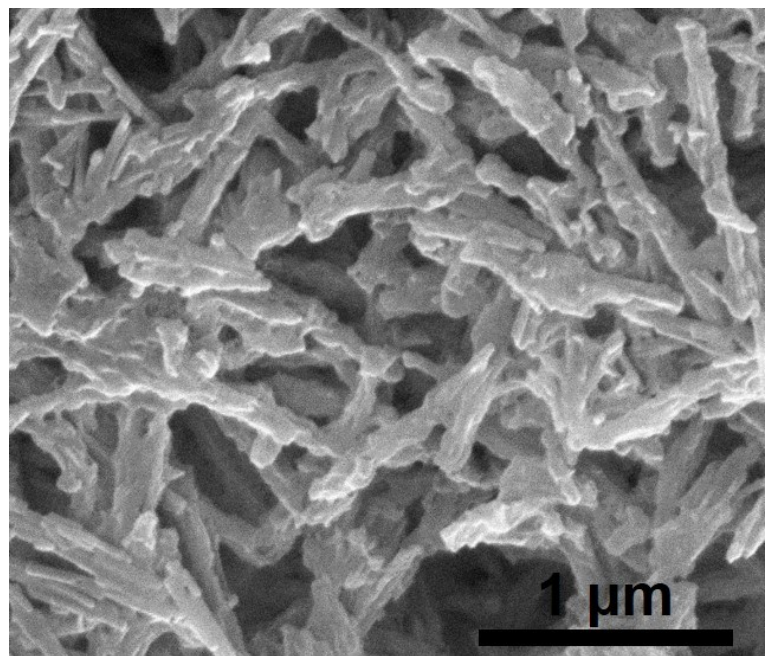


**Fig. S9.** SEM image of CdS/Co(OH)<sub>2</sub> nanocomposites (the order of addition is Co(NO<sub>3</sub>)<sub>2</sub>·6H<sub>2</sub>O first, and then 2MIM).

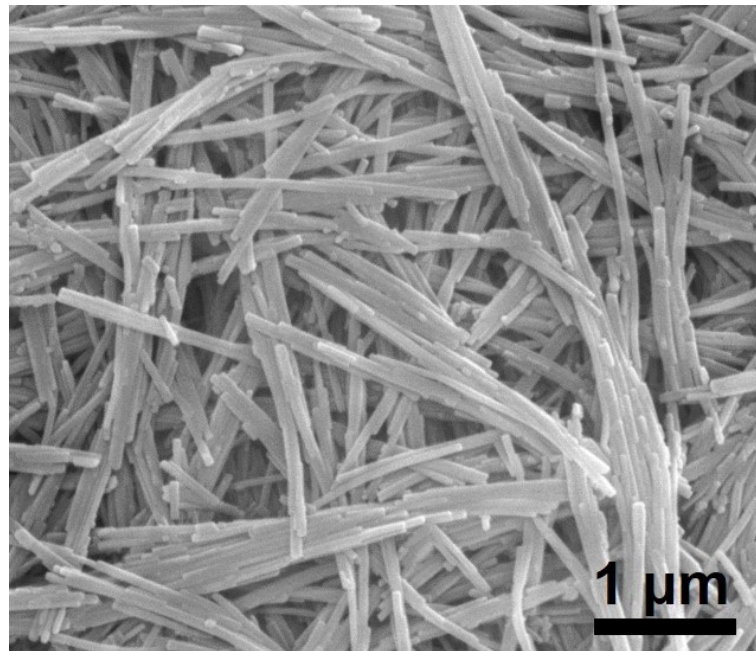


**Fig. S10.** SEM image of CdS/Co(OH)<sub>2</sub> nanocomposites prepare in the anhydrous system, which actually shows that no Co(OH)<sub>2</sub> is formed.

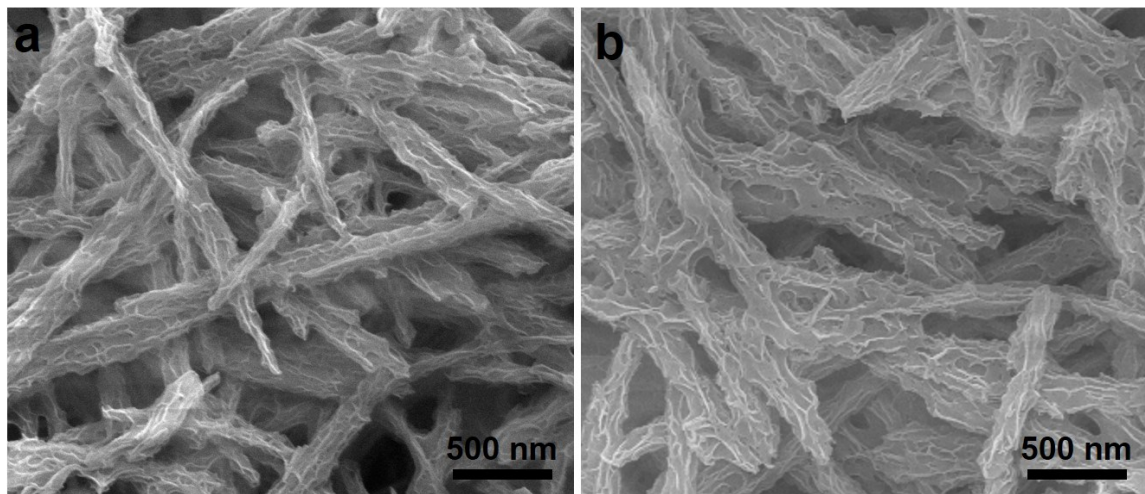


**Fig. S11.** SEM images of CdS/Co(OH)<sub>2</sub> nanocomposites obtained by adding (a) 0.2 and (b) 0.6 mL of water into the anhydrous system, respectively.

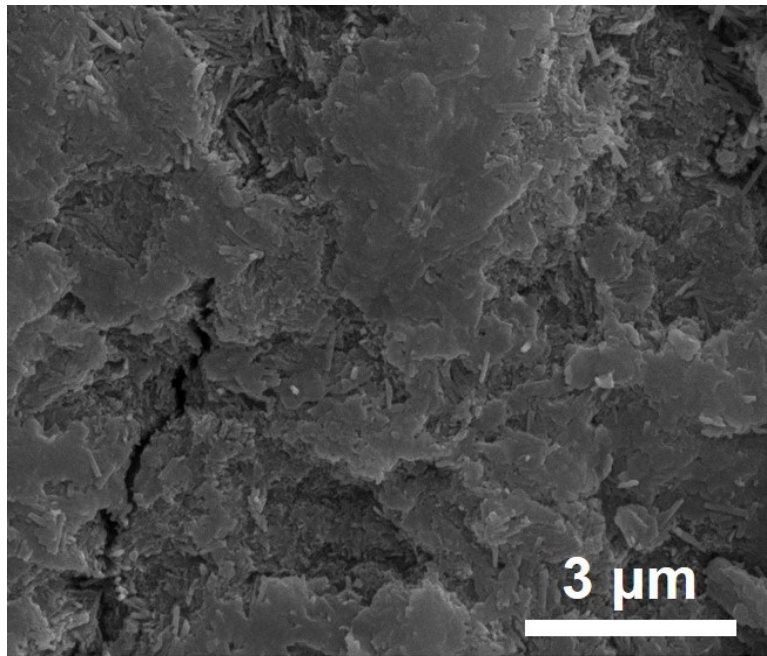


**Fig. S12.** SEM image of CdS/Co(OH)<sub>2</sub> nanocomposites when the reaction solvent is only water.

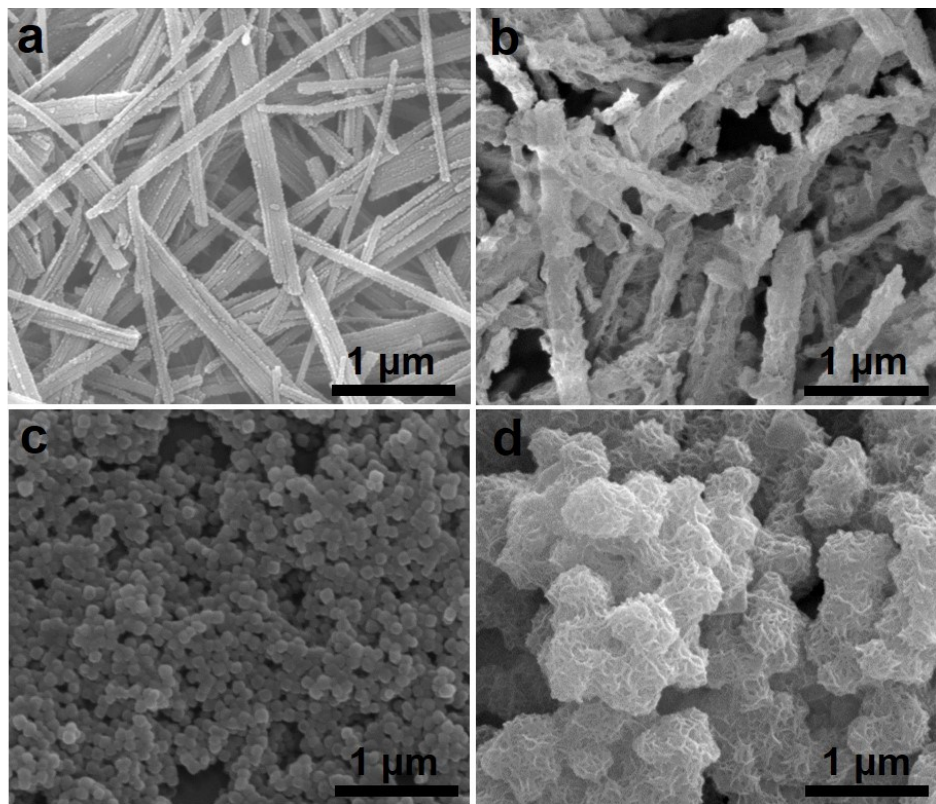


**Fig. S13.** SEM images of (a)  $\text{TiO}_2$  nanobelts, (b)  $\text{TiO}_2/\text{Co}(\text{OH})_2$  nanocomposites, (c)  $\text{Cu}_2\text{O}$  nanoparticles and (d)  $\text{Cu}_2\text{O}/\text{Co}(\text{OH})_2$  nanocomposites.

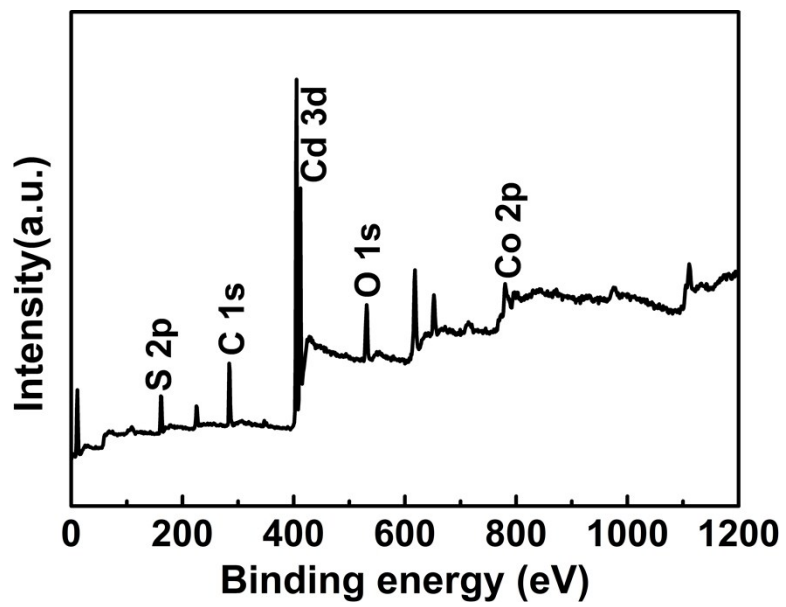


**Fig. S14.** Survey XPS spectrum of CdS/CoO-1h heterostructures, which shows the existence of S, Cd, O, and Co elements.

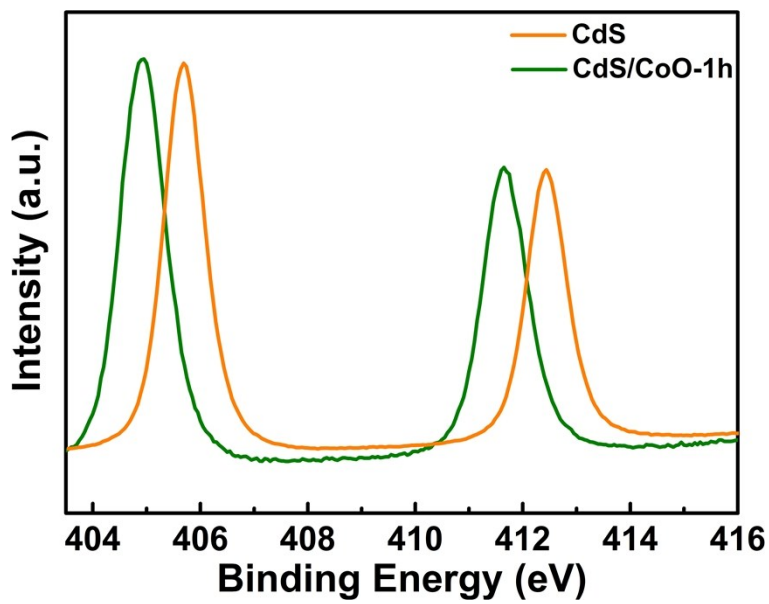


**Fig. S15.** XPS spectra of Cd 3d for CdS nanorods and CdS/CoO-1h heterostructures, which shows shifts to lower binding energies for the CdS/CoO-1h heterostructures and reveals that the electron density of CdS is increased with the decoration of CoO nanoparticles.

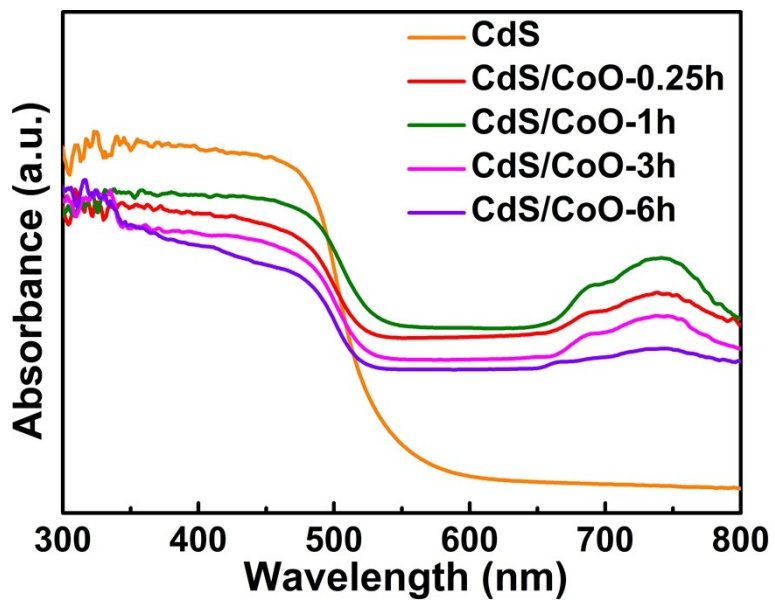


**Fig. S16.** Comparison of UV-vis absorption spectra of the prepared CdS/CoO- $x$ . ( $x=0.25\text{ h}, 1\text{ h}, 3\text{ h}$  and  $6\text{ h}$ )

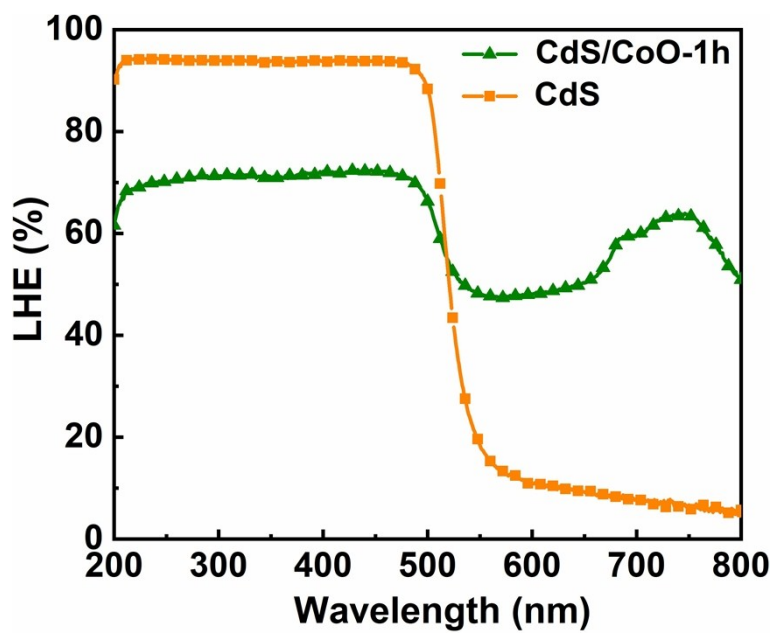


**Fig. S17.** The light harvesting efficiency of the CdS and CdS/CoO-1h heterostructures.

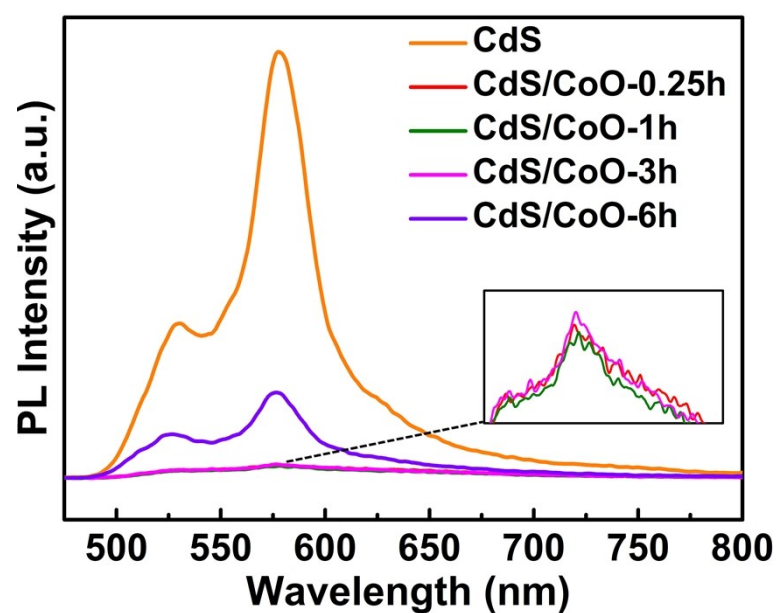


**Fig. S18.** Comparison of PL spectra of the prepared CdS/CoO- $x$ . ( $x=0.25$  h, 1 h, 3 h and 6 h)

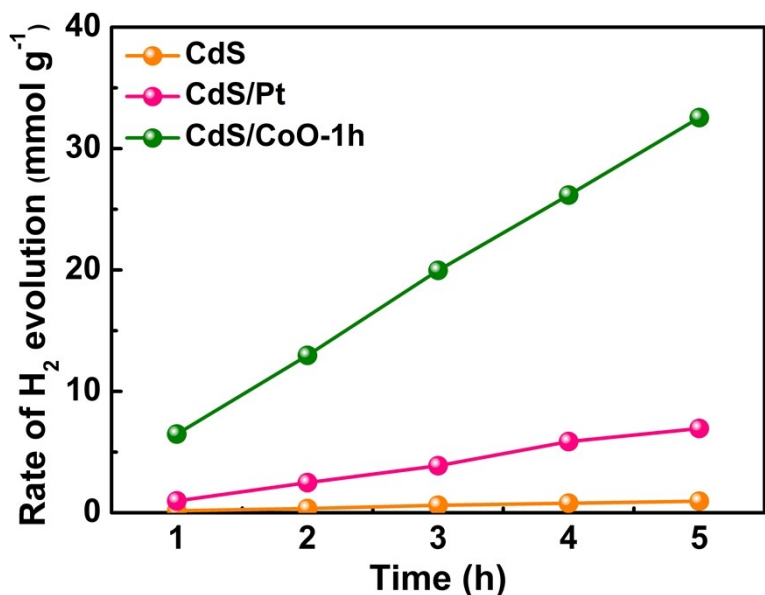


**Fig. S19.** Photocatalytic hydrogen evolution activities of CdS, CdS/Pt and the CdS/CoO-1h heterostructures.

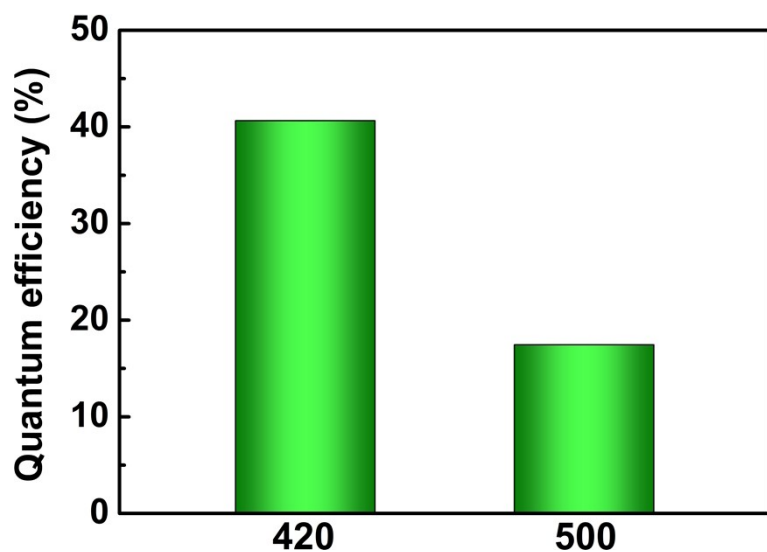


**Fig. S20.** The corresponding apparent quantum yield (AQY) of the Cds/CoO-1h heterostructures.

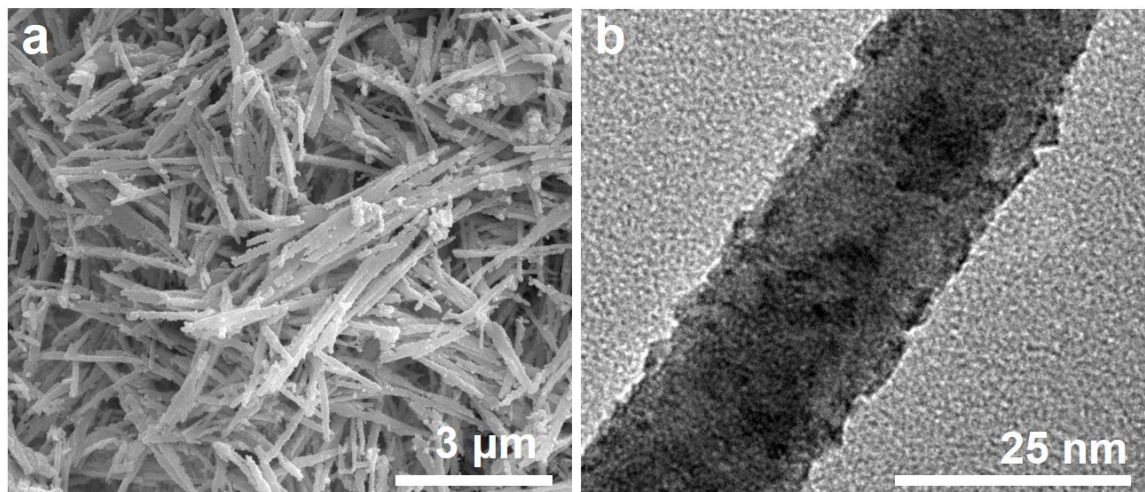


**Fig. S21.** (a) SEM and (b) TEM images of the used CdS/CoO-1h heterostructures, which show no obvious structure collapse during the photocatalytic hydrogen evolution process.

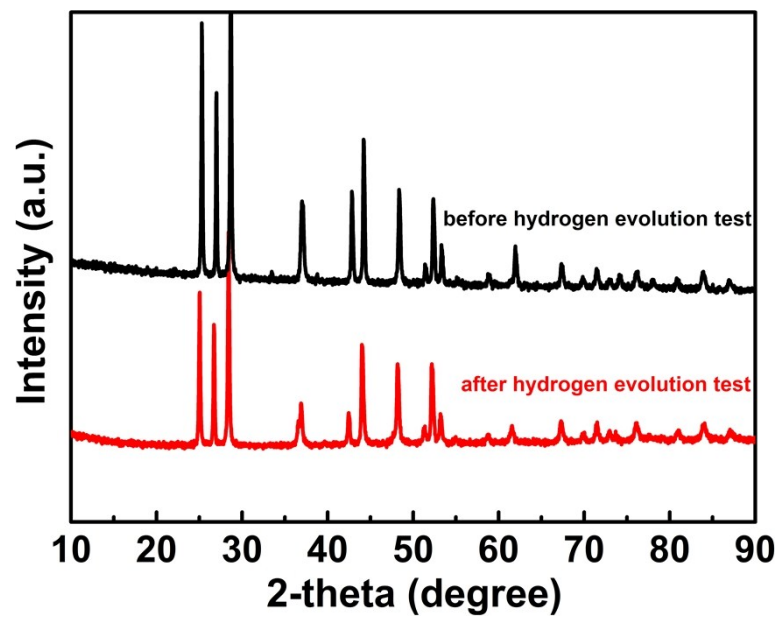


**Fig. S22.** XRD patterns of the CdS/CoO-1h heterostructures before and after hydrogen evolution test.

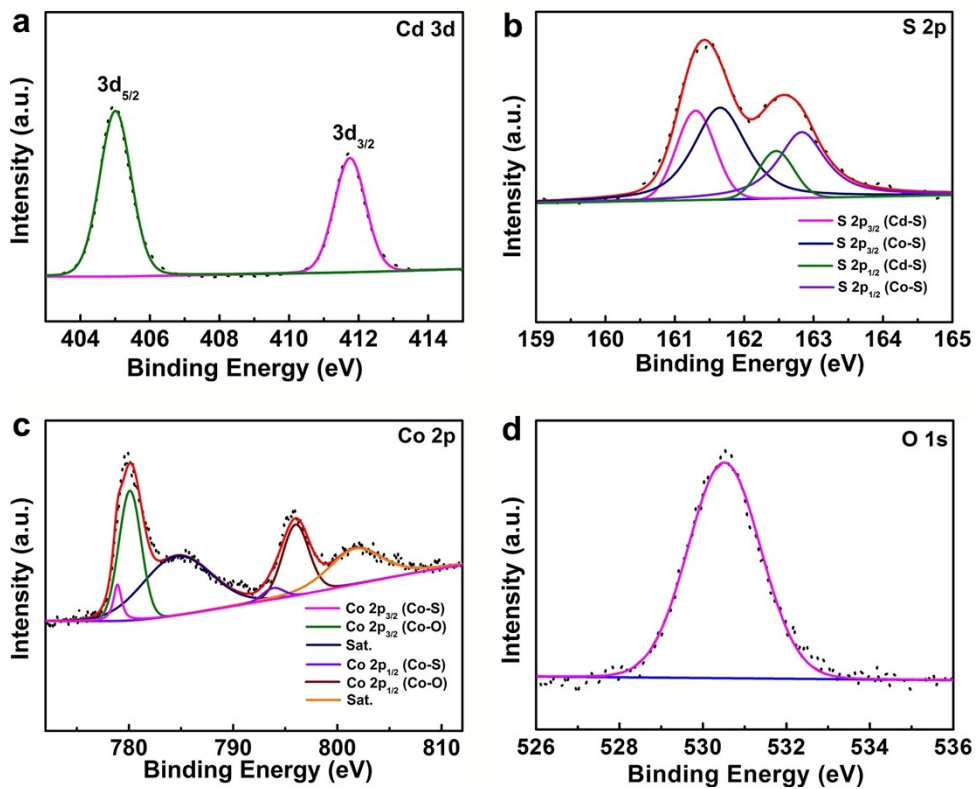


**Fig. S23.** XPS spectra of the used CdS/CoO-1h heterostructures: (a) Cd 3d, (b) S 2p, (c) Co 2p and (d) O 1s. From the S 2p and Co 2p spectra, Co-S bonding features can still be clearly seen, ensuring the stable photocatalytic performance.

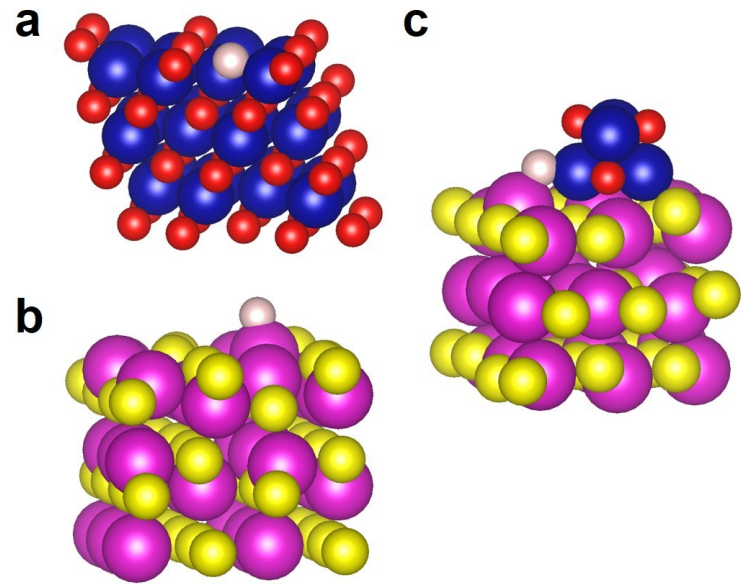


**Fig. S24.** Optimized geometry of H adsorbed structures of (a) CoO, (b) CdS and (c) CdS/CoO with CoO clusters on CdS (100) interface.

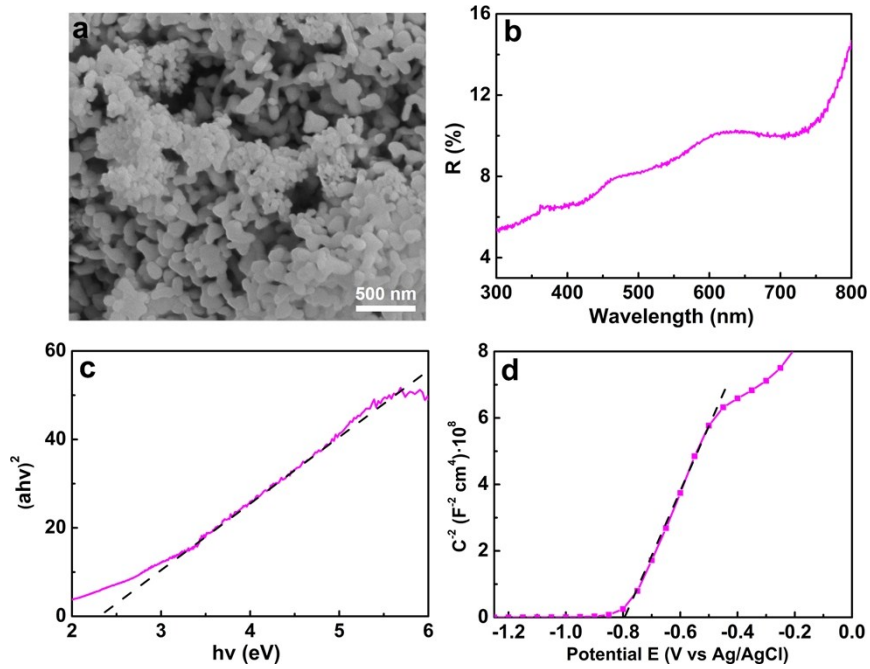


**Fig. S25.** (a) SEM image, (b) ultraviolet–visible diffuse reflectance spectra, (c) optical bandgap and (d) Mott-Schottky plot of commercial CoO nanoparticles.

**Table S1** The molar ratio of Co to Cd in CdS/CoO-x heterostructures determined by XPS and ICP.

Samples	XPS	ICP
CdS/CoO-0.25 h	0.18	0.29
CdS/CoO-1 h	0.73	0.62
CdS/CoO-3 h	1.45	1.33
CdS/CoO-6 h	2.21	2.29

**Table S2** Parameters obtained from time-resolved PL decay curves according to a double-exponential decay.

Samples	$\tau_1$ (ns)	$\tau_2$ (ns)	A <sub>1</sub> (%)	A <sub>2</sub> (%)	lifetime (ns)
CdS	1.28	6.18	39.86	60.14	4.22
CdS/CoO-1 h	1.44	7.89	26.65	73.35	6.17

**Table S3** A brief survey of CdS and CoO hydrogen evolution photocatalysts reported in literature.

Catalyst	H <sub>2</sub> production rate ( $\mu\text{mol g}^{-1}\text{h}^{-1}$ )	Light source (nm)	Cocatalyst	Sacrificial reagent	Ref
CdS/CoO <sub>x</sub>	~3500	350 W Xe lamp ( $\lambda \geq 420$ )		Na <sub>2</sub> SO <sub>3</sub> /Na <sub>2</sub> S	<sup>5</sup>
g-C <sub>3</sub> N <sub>4</sub> /CoO	~650	300 W Xe lamp ( $\lambda \geq 400$ )	3 w% Pt	triethanolamine	<sup>6</sup>
NiS/CdS	~1512	300 W Xe lamp ( $\lambda \geq 400$ )		lactic acid and lignin	<sup>7</sup>
CdS/Ni	~4300	300 W Xe lamp ( $\lambda \geq 420$ )		Na <sub>2</sub> SO <sub>3</sub> /Na <sub>2</sub> S	<sup>8</sup>
CdS/CdIn <sub>2</sub> S <sub>4</sub>	~830	300 W Xe lamp ( $\lambda \geq 420$ )		Na <sub>2</sub> SO <sub>3</sub> /Na <sub>2</sub> S	<sup>8</sup>
CdS/WO <sub>3</sub>	~2900	500 W Xe lamp ( $\lambda \geq 400$ )	3 w% Pt	lactic acid	<sup>9</sup>
Au-CdS	~600	300 W Xe lamp ( $\lambda \geq 420$ )		Na <sub>2</sub> SO <sub>3</sub> /Na <sub>2</sub> S	<sup>10</sup>
CdS/WO <sub>3</sub>	~2900	500 W Xe lamp ( $\lambda \geq 400$ )	3 w% Pt	lactic acid	<sup>11</sup>
Cd/CdS	~2570	300 W Xe lamp ( $\lambda \geq 410$ )		Na <sub>2</sub> SO <sub>3</sub> /Na <sub>2</sub> S	<sup>12</sup>
NiS/carbon dots/CdS	~1450	350 W Xe lamp ( $\lambda \geq 420$ )		Na <sub>2</sub> SO <sub>3</sub> /Na <sub>2</sub> S	<sup>13</sup>
CdS/Zn <sub>x</sub> Co <sub>3-x</sub> O <sub>4</sub>	~4000	300 W Xe lamp ( $\lambda \geq 420$ )		lactic acid	<sup>14</sup>
<b>CdS/CoO</b>	<b>~6450</b>	<b>300 W Xe lamp (<math>\lambda \geq 420</math>)</b>		<b>lactic acid</b>	<b>This work</b>

## Reference

1. B. Ma, H. Xu, K. Lin, J. Li, H. Zhan, W. Liu and C. Li, *ChemSusChem*, 2016, **9**, 820-824.
2. L. Yang, B. Zhang, W. Ma, Y. Du, X. Han and P. Xu, *Mater. Chem. Front.*, 2018, **2**, 1523-1528.
3. D. Gallant, M. Pezolet and S. Simard, *J. Phys. Chem.: B*, 2006, **110**, 6871-6880.
4. W. Shi, F. Guo, H. Wang, S. Guo, H. Li, Y. Zhou, C. Zhu, Y. Liu, H. Huang, B. Mao, Y. Liu and Z. Kang, *ACS Appl. Mater. Interfaces*, 2017, **9**, 20585-20593.
5. Y. Liu, S. Ding, Y. Shi, X. Liu, Z. Wu, Q. Jiang, T. Zhou, N. Liu and J. Hu, *Appl. Catal. B-Environ.*, 2018, **234**, 109-116.
6. Z. Mao, J. Chen, Y. Yang, D. Wang, L. Bie and B. D. Fahlman, *ACS Appl. Mater. Interfaces*, 2017, **9**, 12427-12435.
7. Y. Zhang, Z. Peng, S. Guan and X. Fu, *Appl. Catal. B-Environ.*, 2018, **224**, 1000-1008.
8. G. Zhao, Y. Sun, W. Zhou, X. Wang, K. Chang, G. Liu, H. Liu, T. Kako and J. Ye, *Adv. Mater.*, 2017, **29**, 1703258.
9. R. Li, H. Han, F. Zhang, D. Wang and C. Li, *Energy Environ. Sci.*, 2014, **7**, 1369-1376.
10. P.-Y. Kuang, P.-X. Zheng, Z.-Q. Liu, J.-L. Lei, H. Wu, N. Li and T.-Y. Ma, *Small*, 2016, **12**, 6735-6744.
11. L. J. Zhang, S. Li, B. K. Liu, D. J. Wang and T. F. Xie, *ACS Catal.*, 2014, **4**, 3724-3729.
12. B. Wang, S. He, W. Feng, L. Zhang, X. Huang, K. Wang, S. Zhang and P. Liu, *Appl. Catal. B-Environ.*, 2018, **236**, 233-239.
13. R.-B. Wei, Z.-L. Huang, G.-H. Gu, Z. Wang, L. Zeng, Y. Chen and Z.-Q. Liu, *Appl. Catal. B-Environ.*, 2018, **231**, 101-107.
14. F. Guo, W. Shi, C. Zhu, H. Li and Z. Kang, *Appl. Catal. B-Environ.*, 2018, **226**, 412-420.